Numerical Modeling of Spudcan Footing Penetration in Sand

P. Gütz, K. Abdel-Rahman, M. Achmus

Institute for Geotechnical Engineering
Leibniz University of Hannover, Germany

P. Peralta

Fugro GeoConsulting, Belgium

Abstract: Spudcans are a type of footing foundation to provide a secure operation of mobile jack-up rigs. They are connected to each of the independent legs of a jack-up rig. The current practice to assess the penetration depths of spudcans and the risk of geotechnical failure (punch-through) involves calculating the bearing capacity of the footing at discrete depths. The finite element method offers the possibility to model the complex spudcan penetration process while involving detailed soil parameters and spudcan geometry. In this paper, the use of Coupled Eulerian-Lagrangian (CEL) model elements, available in ABAQUS, to simulate large soil deformations during the spudcan penetration process is described. The novel approach allows the separation of the material movement from the finite element mesh and thus overcomes numerical problems associated with large distortion of elements. This method combines Lagrangian elements, which can represent solid structures (such as a spudcan), with Eulerian elements that idealize the soil. The application of CEL elements in a finite element model of the spudcan penetration process allows large-strain failure mechanisms to be observed, better understood and additionally, the effects of the penetration process to be estimated.

Keywords: Offshore, Spudcan, soil-structure-interaction, Abaqus, Coupled Eulerian-Lagrangian (CEL).

1. Introduction

In this study, the Coupled Eulerian Lagrangian numerical method was applied to simulate the spudcan penetration process. The set up of the CEL model of a spudcan is described and afterwards validated against published work of Qiu & Henke (2011) and Qiu et al. (2011a). The numerical results of the analysis are subsequently presented.

Spudcans are used as footing foundations providing a secure operation of mobile jack-up rigs. The legs of the rig are jacked into the seafloor to hold the rig in its position and ensure stability against horizontal and vertical forces. These rigs are widely operating in the offshore industries such as oil and gas exploration for drilling wells, maintenance work or temporary production. Further application of mobile jack-up rigs can be observed in the emerging field of offshore renewable energy, for the erection of offshore wind energy plants.

The diameter of spudcans usually range between 10 m and 16 m but are steadily increasing, exceeding 20 m in recent years. In general, spudcans are approximately circular in plan but may also have a polygonal shape and mostly have a conical underside (about 15° to 30° to the horizontal). Additionally, a spudcan can incorporate an acute tip called spigot centered on the bottom, which improves its sliding resistance. The top face also exhibits a conical shape with angle to the horizontal similar to the one of the underside (Hossain & Randolph, 2010a). Figure 1 depicts a typical shape of a spudcan-footing.

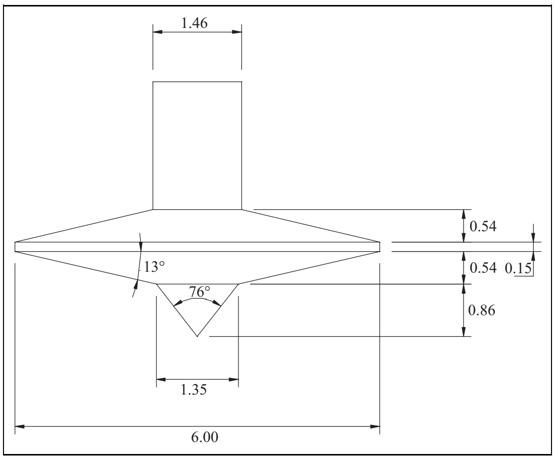

Figure 1: Typical geometry (in [m]) of a spudcan (Hossain & Randolph, 2010a)

Guidelines on the site specific assessment of jack-up rigs and its components are provided in the International Standard ISO 19905-1:2011 and in the Technical and Research Bulletin 5-5A of the Society of Naval Architects and Marine Engineers (SNAME, 2008). Further guidelines on geotechnical assessments including foundation design can be found in ISO19901-4:2003.

2. Overview of Previous Work

Spudcan footings for jack-up rigs have been used in the oil and gas industry for the past 30 years. Experience gained from practice as well as research applying model tests have shown that the penetration depth of spudcans in sand layers is shallow, not normally exceeding the height of the spudcan. In contrast, the penetration depth of a spudcan in soft clay can reach a depth several times its diameter.

Recent model tests and numerical simulations have confirmed the above observation. Tho & Leung (2011) observed that a spudcan penetrates only at shallow depth in sand or stiff clay so that the edge of the spudcan is still above or slightly below the original seabed.

The penetration depth, and hence the penetration resistance, of a spudcan depends significantly on whether the the soil is drained or undrained during the process. Usually, it is assumed that penetration in sand is a drained process, whereas in cohesive soils such as clay, penetration may be assumed to be an undrained process (ISO 19905-1:2011). In addition to the general soil type, drainage conditions during penetration are also influenced by the rate of spudcan penetration. The increase of the penetration rate leads to enlarged undrained behaviour of the soil and thus to a decrease of penetration resistance (Houlsby & Cassidy, 2011). This association is depicted in Figure 2. However, it should be noted that a further increase of the penetration rate beyond the fully undrained state leads to viscous effects as well as enlarged strain rates, which will also increase the penetration resistance (Lee & Randolph, 2011).

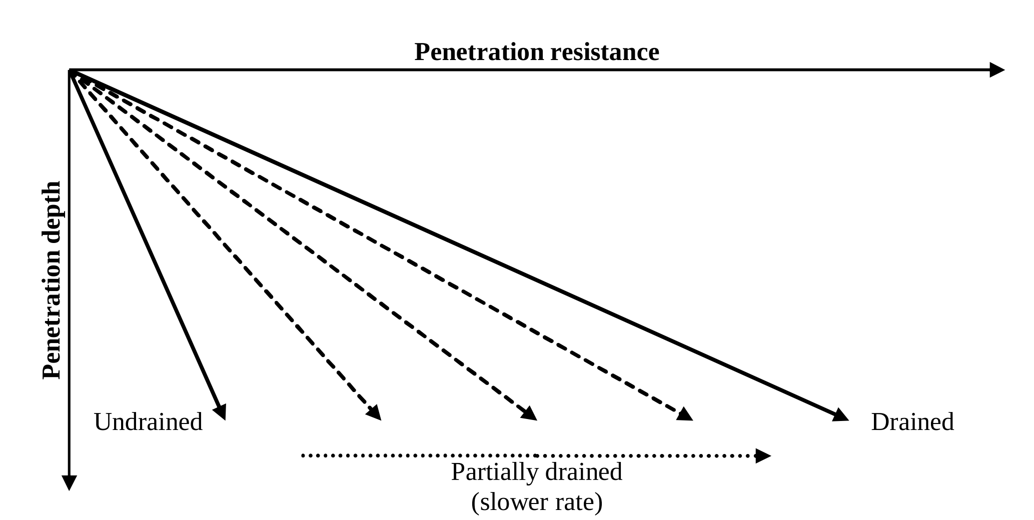

Figure 2: Penetration resistance as function of the penetration rate adapted from Houlsby & Cassidy (2011)

Analytical methods to assess the spudcan penetration depth apply simple models that idealize the complex spudcan penetration process. Except for some new mechanism based approaches, most of the models applied for spudcans have been based on theories developed for shallow foundations and thus do not consider the actual progress of spudcan penetration with depth. These analytical methods for spudcan penetration assessment may have significant limitations especially when encountering complex soil conditions, such as layered soil profiles (Kellezi & Stromann, 2003).

In recent years, the assessment of spudcan penetration has been investigated applying numerical methods. Classic Finite Element Analysis (FEA) methods using Lagrangian elements have been used to model a spudcan. However, such analysis using Lagrangian elements are limited to small-deformation problems. As the spudcan penetrates further in to the soil, large deformations of model elements occur leading to numerical and convergence problems. The large deformations in the model cause significant distortions of the mesh and its elements as well as contact problems between the spudcan and the soil (Qiu, et al., 2011a). Hossain et al. (2005) attempted to overcome this limitation by simulating with pre-embedment of the spudcan at a certain depth.

More recently, FEA methods using an Arbitrary Lagrangian- Eulerian (ALE) formulation process have been investigated and successfully applied to large-deformation problems, such as spudcan penetration. Results of such analysis have been shown to be in agreement with model tests (Hossain & Randolph, 2010b; Gao, et al., 2012).

Another method, using Coupled Eulerian-Lagrangian (CEL) elements in ABAQUS, has been shown to be able to model large-deformation problems. Tho et al. (2009) first applied the CEL method for the assessment of spudcan penetrations. This approach has since been benchmarked and validated for application in other large-deformation, geotechnical problems (Qiu, et al., 2009; Qiu, et al., 2011b). There are several other recent publications documenting the applicability of the CEL method for spudcan penetration assessments (Qiu & Henke, 2011; Tho, et al., 2012; Yi, et al., 2012).

The next section describes the CEL formulation, which is subsequently applied in a numerical model to investigate the spudcan penetration process in sandy soil.

3. Coupled Eulerian-Lagrangian Method

There are two ways to describe the movement of a certain volume as a function of time, namely the Lagrangian and Eulerian description. In the Lagrangian description, the movement of material is a function of the material coordinates and time (Qiu et al., 2011b). The nodes of a Lagrangian mesh are bound to the material and the mesh deforms simultaneously as the material deforms. A Lagrangian element is always completely filled with a single material and its boundary represents the material boundary (Simulia, 2012). Thus, the contact interface between two materials is precisely defined. Due to the precise material boundaries and contact interface, simulation of large-deformation problems producing high distortion of the mesh and elements negatively impacts the accuracy of the calculation. Numerical errors such as stress concentrations, singular plasticity and high-velocity gradients may occur leading to convergence problems (Simulia, 2012).

In the Eulerian description, the movement of material is a function of the spatial coordinates and time (Qiu, et al., 2011b). The nodes of a Eulerian mesh are fixed in space and the material flows through the elements. The material boundaries in a Eulerian element are not precisely defined so that an element can contain more than one material at the same time or contain a full or partial void. Since the nodes of the mesh are not bound to the material, the elements in a mesh remain undistorted as the material moves. Numerical simulations requiring large material movement can be performed without causing convergence problems associated with high element distortions.

However, material boundaries including interfaces between multiple materials within an element have to be computed in each time increment (Qiu, et al., 2011a; Simulia, 2012). Thus, accurate calculation of material location requires fine meshes and simple geometries. A disadvantage of the Eulerian analysis is the occurrence of numerical diffusion that leads to increasingly inaccurate results with advancing simulation period.

The CEL method in ABAQUS combines the advantages of Eulerian and Lagrangian elements to analyze problems involving both small and large deformations, which is generally not feasible with conventional Lagrangian FEA methods. In geotechnical applications, the CEL method allows the soil, which may undergo large deformations, to be modeled using Eulerian elements while solid structures with little deformations can be modeled using Lagrangian elements. Numerical convergence problems associated with stress and strain concentrations at the edge of a solid structure are overcome since the Eulerian soil element is able to move freely.

The interface between the two elements defines the boundary of the Lagrangian body. The Lagrangian body occupies a region in the Eulerian mesh, while it pushes the Eulerian material out of the elements since there is no material flow of Eulerian material in the Lagrangian body (Tho et al., 2012). This process is calculated with a time incrementation algorithm that consists of a traditional Lagrangian phase followed by a Eulerian transport phase.

The CEL method is particularly advantageous in simulating installation processes in geotechnical engineering, which typically involve large soil deformations. The installation of foundations, such as piles and/or footings, can be simulated realistically beginning at the ground surface in contrast to modeling pre-embedded foundations (Qiu, et al., 2009).

4. Development of the CEL Model

The spudcan penetration analysis under purely vertical loading is an axisymmetric process, which could, in principle, be analyzed as a two-dimensional problem. However, ABAQUS provides only one Eulerian element type that is a 3D element requiring eight nodes. Therefore, a 3D model of the spudcan and soil mass was created in this study; however, the model was optimized by utilizing symmetry. Two planes of symmetry were established and only one-fourth of the spudcan and soil domain was modeled (see Figure 3). Boundary conditions were applied to the planes of symmetry, which inhibit material movement normal to the planes of symmetry. The type of boundary condition in the ABAQUS model was set to “no-flow-boundaries”. This type of boundary condition enforces zero velocity in the boundary, in the direction of the given boundary condition.

The dimension of the complete model was based on numerical studies of Qiu & Henke (2011). However, the applied spudcan geometry was based on the models of Craig & Chua (1990) and Qiu et al. (2011a).

The model contains a spudcan with radius 7 m and a soil domain with radius 28 m, which is equal to four times the spudcan radius (Figure 3). The horizontal dimension of the soil model is thus expected to be large enough to avoid any boundary effects. The height of the soil model was increased to 56 m, which is equal to four times the diameter of the spudcan. This allows penetration of the spudcan up to a multiple of its diameter without boundary effects. In addition, an initial void region above the soil mass provides enough space for the soil heave.

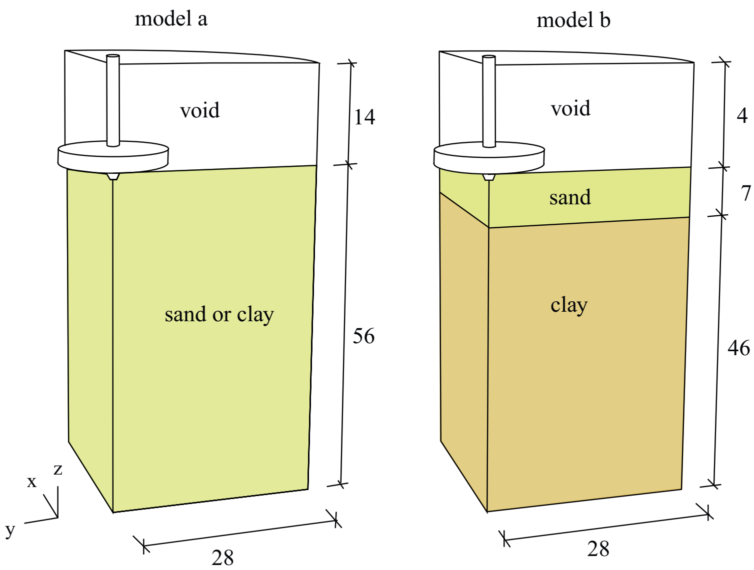

Figure 3: Dimensions and geometry of spudcan penetration model

In the CEL model, the soil mass and initial void regions above the soil were assigned with Eulerian elements while the spudcan itself was assigned with Lagrangian elements. The model was made up of several parts, with the element size of the mesh adjusted for each part. A fine mesh was applied in proximity to the spudcan while a coarser mesh was applied to the model parts close to the boundaries. This allowed an optimization of total number of elements in the model without compromising on accuracy of calculated soil movements in proximity to the spudcan.

The soil mass was assigned as either sand or clay. In some models, the soil mass consisted of layered sand and clay (Figure 3). The Mohr-Coulomb plasticity constitutive law was chosen to represent the behavior of sand. Table **1**contains the required soil properties for the Mohr-Coulomb constitutive law that was applied in the model. The soil properties for sand were mainly adopted from the model of Qiu & Henke (2011) to enable comparison of results. A negligible value of cohesion was assumed to overcome numerical instabilities.

Table **1: Applied soil properties for sand**

Parameter	Value
Unit weight	11 KN/m^3
Young's modulus	50.0 MPa
Poisson's ratio	0.25
Friction angle	38.0°
Dilatation angle	8.0°
Cohesion	0.01 kPa

Since the elements of the Eulerian mesh may not be always full of one material, ABAQUS uses the corresponding volume fraction of the material to determine average state variables, such as stresses and strains (Simulia, 2012).

Spudcans are constructed from steel and are hollow. In the CEL model, the equivalent density of the spudcan is 2.0 t/m^3. However, since the deformation of the spudcan is of minor interest in the analysis, the spudcan was modeled as a rigid body using Lagrangian elements. The rigid body is assigned to a reference point on the spudcan, where the boundary conditions and the output requests are applied on.

ABAQUS provides the general contact method to define the interaction between the Lagrangian and Eulerian material, which allows finite sliding of two separated surfaces. This aspect is essential for the spudcan penetration analysis, where the soil continuously moves along the spudcan surface. The definition of a friction coefficient represents the roughness of the spudcan surface. The interaction property is stated as a penalty contact with a friction coefficient of 0.5 (equals δ=26.57°). The general contact is required in the CEL analysis with Abaqus.

The numerical analysis is generally performed in two steps. The initial step defines the geostatic stress field, which is induced by self-weight of the soil under gravity. The second step applies loads in the model to initiate the analysis and includes the spudcan penetration process. This step is a dynamic, explicit type analysis. A displacement-controlled force with a constant penetration rate was applied to the spudcan in the model. The time period of the step was defined in relation to the penetration rate of the spudcan and penetration depth to be reached (with penetration depth/time period = penetration rate).

In addition to the boundary conditions defining the planes of symmetry, another boundary condition was specified to apply the penetration rate or velocity of 0.5 m/s to the spudcan. A pre-defined field to establish the initial velocity of the same magnitude to the spudcan was also defined in the initial step.

4.1 Validation and Convergence Study

The element size of the mesh for each part of the model was optimized with the aim to create approximately 50,000 elements for best comparison with the results of Qiu and Henke (2011). Initially, global seeds with an approximate element size of 1 m were applied. Seeds with a size-dependent bias were afterwards selected to produce a very fine mesh region in proximity to the spudcan and a coarser mesh near the bottom of the model for computational efficiency.

The final model described in this paper contains 59,455 elements. The smallest element size is 0.25 m near the spudcan, but increases in size in both horizontal and vertical directions towards the model boundaries. A global seed size 0.5 m was chosen.

An initial simulation of the spudcan penetration process, replicating the model of Qiu & Henke (2011), was carried out to verify the numerical model. Figure 4 presents the results of the numerical simulation in comparison to those of Qiu & Henke. The results compare the bearing pressure of the spudcan with penetration depth and show a very good fit between the two models. There is a slight mismatch in the penetration range of 0 m to 1.50 m with a difference of 12 % at most. After 1.50 m penetration depth, both graphs are nearly identical.

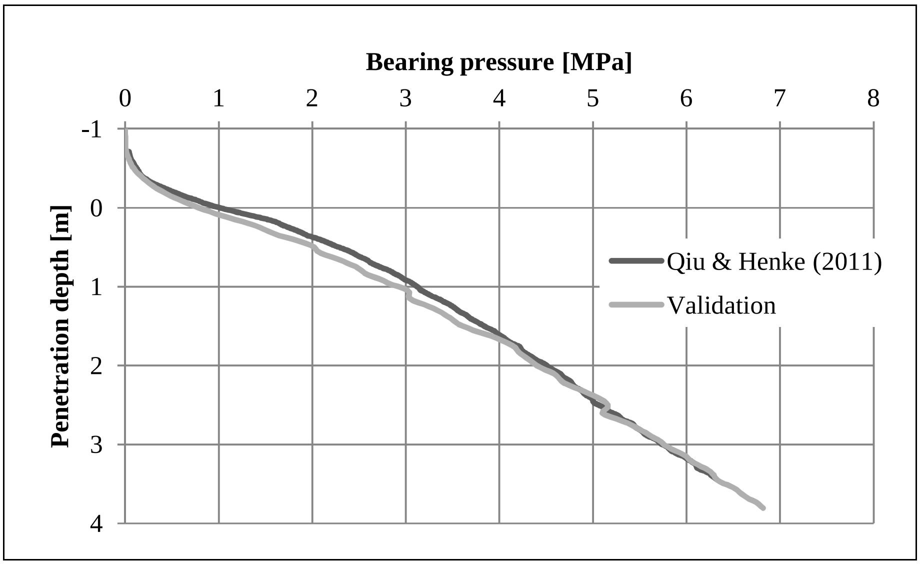

Figure 4: Bearing pressure of a spudcan penetrating into uniform sand; comparison to Qiu & Henke (2011)

Based on the validation of the model, a convergence study on the mesh density as well as the penetration velocity was performed. Different meshes with varying the number of elements as well as the minimum element size were investigated (see Table 2). Figure 5 presents the results of the spudcan penetration analysis in terms of bearing pressure with penetration depth, applying different mesh sizes. The comparison reveals no substantial differences in the calculated resistance of the spudcan due to mesh density. However, bearing pressure graphs are much smoother (without excessive instabilities) as the number of elements in the model is increased. Since there were no significant differences between mesh B, C and D, mesh B with total element number 100,536 was chosen for all subsequent analysis to optimize accuracy and computational time. The numerical modeling was done using the computer server with Intel Xeon X5670, 2.93 GHz processor with a main memory of 48 GB. The number of cores used is 8.

Table 2: Mesh densities applied in convergence study

	Mesh A	Mesh B	Mesh C	Mesh D
Number of elements	59,455	100,536	150,960	255,668
Minimum element size [m]	0.25	0.2	0.15	0.15
CPU time (approximately) [h]	2	4	10	17

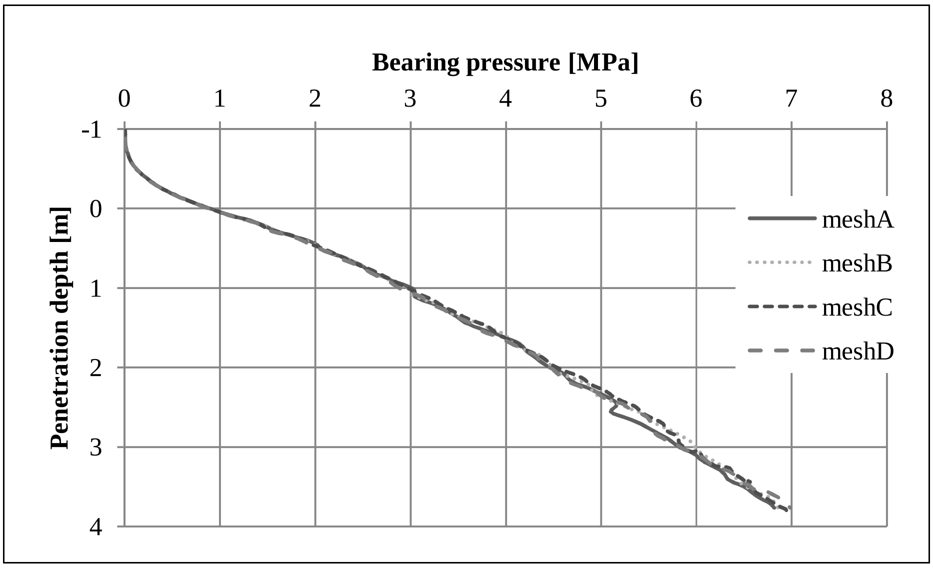

Figure 5: Convergence study on the mesh density

The effect of the penetration rate on the spudcan bearing resistance was also investigated. In a numerical model, the penetration rate is much faster compared to the actual penetration rate in-situ, which may take up to 1 day or 3 days depending on soil conditions. Thus, this divergence from real conditions must be taken into consideration. Figure 6 depicts the results of the simulations with different applied penetration rates. The results indicate that an increasing penetration rate leads to a slightly higher bearing capacity. The bearing capacity graphs show an increasing instability with higher penetration rate and advancing penetration (compare graphs with penetration rates of 0.5 m/s and 1 m/s). The analysis with penetration rate 0.1 m/s was aborted due to exceedance of CPU time (> 59 h at D = 2 m) at approximately 2 m penetration depth (see red curve in Figure 6). The analysis with penetration rate 0.25 m/s produced a smooth graph, which is almost identical to the results with penetration rate 0.1 m/s until it was aborted. Regarding the computational effort, it was observed that the CPU time required increased with decreasing penetration rate, especially for penetration rates less than 0.25 m/s. Hence, a penetration rate of 0.25 m/s was adopted for all subsequent analyses. For more detailes, pl. refer to (Gütz 2012).

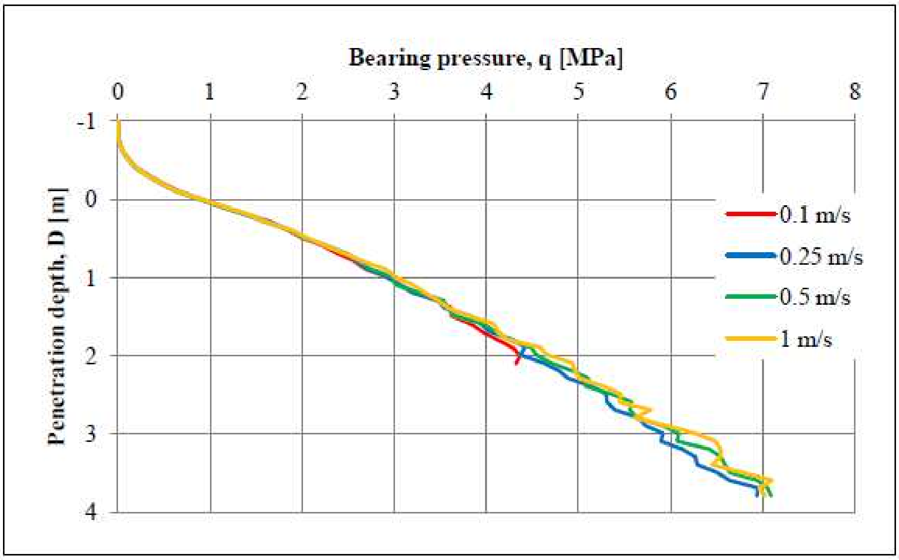

Figure 6: Convergence study on penetration rate in sand

5. Numerical Results

The numerical results of the spudcan penetration analysis were compared to results from analytical methods. Analytical methods to estimate the spudcan penetration depth were applied using Fugro in-house software. Figure 7 depicts the comparison of numerical and analytical results in terms of spudcan reaction versus penetration depth in sand. For all results, it can be observed that the progressively increasing bearing area during partial penetration causes a significant increase of the spudcan reaction for penetration depth D < 0 m. At D = 0 m, the slope of the curves increases since the bearing area does not increase further for the embedded spudcan.

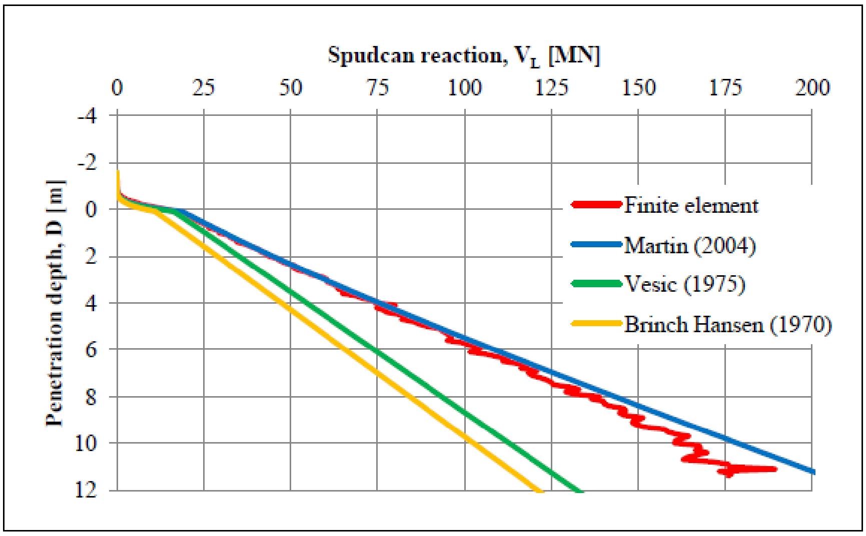

Figure 7: Comparison of finite element and analytical results

Based on general bearing capacity equations (for shallow foundations), the bearing capacity of a spudcan penetrating in cohesionless soil can be separated into two terms: the resistance due to soil weight beneath the footing and the surcharge of the soil above the spudcan (Cassidy & Houlsby, 2002).

For the spudcan at ground surface, the methods of Vesic (1975) and Martin (2004) result in similar spudcan reactions, which are in good agreement with the FE result. The method of Brinch Hansen (1970) exhibits the lowest bearing capacity at ground surface and thus significantly underestimates the results from FE analysis. The increase of spudcan reaction with advancing penetration depth is similar in Vesic's and Brinch Hansen's approach, but lower than the one of Martin. The bearing capacity reaction determined with Martin's method is almost identical with FE results up to penetration D = 4 m (during partial spudcan embedment or penetration). At penetration depth D > 4 m (at deeper penetration), the bearing capacity results of the FE analysis becomes slightly lower than the results applying Martin's method.

Figure 8 illustrates the soil movement induced by the spudcan penetrating in the sandy soil at penetration depth D = 2.95 m. Although soil backfill sets on, the soil movement still reaches the ground surface and indicates a shallow failure mechanism (known as general shear). It could be observed that as the spudcan penetrates deeper into the sand layer, the shallow failure mechanism becomes less obvious. At penetration depth D > 5.50 m, the shallow failure mechanism cannot be observed in the FE model as it transitions to a deep failure mode. At this depth, the increase of spudcan reaction reduces and deviates slightly from the analytical result of Martin (2004) (see Figure 7). For further results, pl. refer to (Gütz 2012).

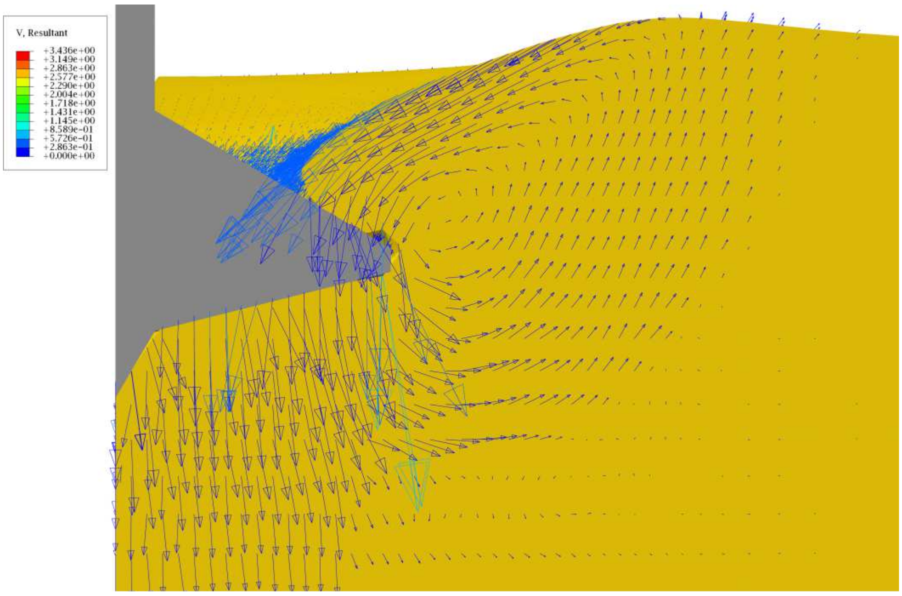

Figure 8: Soil movement [m/s] at penetration depth D = 2.95 m

6. Conclusions

The aim of this paper was to conduct analyses of the spudcan penetration process using a novel finite element approach and to compare these results with the methods that represent the current practice of spudcan penetration analysis. The current standards and guidelines recommend analytical methods to assess the spudcan penetration that are, in general, based on the general bearing capacity approach for shallow foundations.

An essential aspect is the application of the Coupled Eulerian-Lagrangian method in the numerical model, which is suitable for analysis of large deformation problems. The implementation of this finite element model using CEL was validated with previous studies on spudcan penetration analyses. A numerical study was performed that aimed at comparing analytical and finite element results for multiple cases and investigated the effects or mechanisms that occur as the spudcan penetrates in sandy soil.

The comparison of both approaches revealed that the analytical methods applied in practice to estimate the spudcan penetration depth generally match with finite element results, although it was observed that the results of the applied analytical methods mostly underestimated the results from the FE model.

To improve the reliability of the relatively novel CEL method for use in geotechnical applications, further studies comparing model tests and in-situ data with such simulation are highly useful. The continual verification of FE results with model tests, as well as a better understanding and consequently prevention of numerical instabilities will greatly improve the applicability of finite element methods to investigate and analyze the spudcan penetration process. Further potential applications of the CEL method are the investigation of more complex conditions, such as multilayered soil conditions with varying soil properties.

7. References

Brinch Hansen, J., 1970. A revised and Extended Formula for Bearing Capacity. *The Danish Geotechnical Institute Bulletin,* Band 28, pp. 5-11.

Cassidy, M. J. & Houlsby, G. T., 2002. Vertical bearing capacity factors for conical footings on sand. *Géotechnique,* 52(9), pp. 687-692.

Craig, W. H. & Chua, K., 1990. Deep penetration of spud-can foundations on sand and clay.*Géotechnique,* 40(4), pp. 541-556.

Gao, W., Yu, L. & Hu, Y., 2012. Large deformation FE analysis of large diameter spudcan penetration into two-layer of uniform clays. *International Journal of Geotechnical Engineering,* 6(2), pp. 171-177.

Gütz, P, 2012 . Finite Element Analysis of Spudcan Penetration Analysis, Master thesis, Leibniz University of Hannover (unpublished).

Hossain, M. S., Hu, Y., Randolph, M. F. & White, D. J., 2005. Limiting cavity depth for spudcan foundations penetrating clay. *Géotechnique,* 55(9), pp. 679-690.

Hossain, M. S. & Randolph, M. F., 2010a. Deep-penetrating spudcan foundations on layered clays: centrifuge tests. *Géotechnique,* 60(3), pp. 157-170.

Hossain, M. S. & Randolph, M. F., 2010b. Deep-penetrating spudcan foundations on layered clays: numerical analysis. *Géotechnigque,* 60(3), pp. 171-184.

Houlsby, G. T. & Cassidy, M. J., 2011. A simplified mechanically based model for predicting partially drained behavior of penetrometers and shallow foundations. *Géotechnique Letters,* 1(3), pp. 65-69.

ISO 19901-4:2003, 2003. *Petroleum and natural gas industries — Specific requirements for offshore structures — Part 4: Geotechnical and foundation design considerations,* s.l.: International Organization for Standardization.

ISO 19905-1:2011, 2011. *Petroleum and natural gas industries — Site-specific assessment of mobile offshore units — Part 1: Jack-ups,* s.l.: International Organization for Standardization.

Kellezi, L. & Stromann, H., 2003. *FEM analysis of jack-up spudcan penetration for multi-layered critical soil conditions.* Dundee, BGA International Conference on Foundations, pp. 411-420.

Lee, J. & Randolph, M., 2011. Penetrometer-Based Assessment of Spudcan Penetration Resistance. *Journal of Geotechnical and Geoenvironmental Engineering,* 137(6), pp. 587-596.

Martin, C. M., 2004. *User Guide for ABC – Analysis of Bearing Capacity,* University of Oxford: Department of Engineering Science.
Qiu, G. & Henke, S., 2011. Controlled installation of spudcan foundations on loose sand overlying weak clay. *Marine Structures,* Band 24, pp. 528-550.
Qiu, G., Henke, S. & Grabe, J., 2009. *Applications of Coupled Eulerian-Lagrangian Method to Geotechnical Problems with Large Deformations.* London, Simulia Customer Conference.
Qiu, G., Henke, S. & Grabe, J., 2011a. *3D FE analysis of the installation process of spudcan foundations.* London, 2nd International Symposium on Frontiers in Offshore Geotechnics.
Qiu, G., Henke, S. & Grabe, J., 2011b. Application of a Coupled Eulerian–Lagrangian approach on geomechanical problems involving large deformations. *Computers and Geotechnics,* 38(1), pp. 30-39.
Simulia, 2012. Abaqus 6.12
Skempton, A. W., 1951. *The Bearing Capacity of Clays.* London, Building Research Congress.
SNAME, 2008. *Guidelines for Site Specific Assessment of Mobile Jack-Up Units. Technical and Research Bulletin 5-5A,* New Jersey: The Society of Naval Architects and Marine Engineers (SNAME).
Tho, K. K., Leung, C. F., Chow, Y. K. & Swaddiwudhipong, S., 2012. Eulerian Finite-Element Technique for Analysis of Jack-Up Spudcan Penetration. *International Journal of Geomechanics,* 12(1), pp. 64-73.
Tho, K. K., Leung, C. F. & Swaddiwudhipong, S., 2009. *Application of eulerian finite element technique for analysis of spudcan and pipeline penetration into the seabed.* London, 12th International Jack-up Conference.
Vesic, A. S., 1975. Bearing Capacity of Shallow Foundations. In: H. F. Winterkorn & H. Y. Fang, Hrsg. *Foundation Engineering Handbook.* New York: Van Nostrand Reinhold, pp. 121-147.
Yi, J. T. et al., 2012. Eulerian finite element analysis of excess pore pressure generated by spudcan installation into soft clay. *Computers and Geotechnics,* Band 42, pp. 157-170.